

Article

Integrated Characterization of Mudstones in the Andes of Colombia: Understanding Its Complexities for Risk Mitigation

German Alfonso Reyes-Mendoza ^{1,2,*} , José Antonio Henao-Martínez ³ and Eduardo Castro Marín ⁴ 

¹ Maestría en Geotecnia, Escuela de Ingeniería Civil, Universidad Industrial de Santander, Bucaramanga 680002, Colombia

² Facultat de Ciències de la Terra, Universitat de Barcelona, 08193 Barcelona, Spain

³ Escuela de Química, Universidad Industrial de Santander, Bucaramanga 680002, Colombia

⁴ Servicio Geológico Colombiano, Bogotá 111321, Colombia

* Correspondence: georeycol@yahoo.es

Abstract: This article presents a comprehensive vision of particularities and constraints of the Paja Formation in the Northern Andes of Colombia, supported by personal, institutional, and academic experiences, including a doctoral thesis in completion (geomorphology and risks research line). Such fine-grained marine rocks cause severe damage in diverse zones, with little spread, and are very unfavorable, especially within the Eastern Cordillera (departments of Santander and Cundinamarca), whose socio-environmental problems motivated a popular legal action in the municipality of Vélez due to the cracking and collapse of houses, damage to roads and landslides in the urban area, as well as flows, subsidence, and high hydrogeochemical dynamism or rare earths, although they also presented spontaneous ignition at the rural area. Understanding how these problems originate and interrelate is the main objective of the work. At the beginning, we include some brief definitions, terms, and key approaches to understand the consolidated geomaterials, location, and background of the problem; then, the results of meso–macro–micro studies, obtained by combining the field techniques and conventional instrumental laboratory analyses (tests on the chemistry of water and soil, description of samples with magnifying glasses, petrography with a polarized light microscope, micromorphology of regoliths–colluvions) of nanoscientists (emphasizing RXD-RXF, SEM, IR-Raman spectroscopy, TOC-TS) are presented. These characterizations and new knowledge must be socially and institutionally appropriated and applied in land use planning and risk management for the sustainability of challenging environments with the stratiforms of Lower Cretaceous rocks and associated Quaternary deposits in populated mountainous areas and contrasting intertropical hydroclimatological regimes, geologically active, so unstable and insecure.

Keywords: mudstones; Andean Cretaceous; material science; weathering; urban geohazards



Citation: Reyes-Mendoza, G.A.; Henao-Martínez, J.A.; Marín, E.C. Integrated Characterization of Mudstones in the Andes of Colombia: Understanding Its Complexities for Risk Mitigation. *Micro* **2023**, *3*, 62–83. <https://doi.org/10.3390/micro3010007>

Academic Editor: Isabelle Huynen

Received: 30 December 2022

Revised: 17 January 2023

Accepted: 17 January 2023

Published: 23 January 2023



Copyright: © 2023 by the authors. Licensee MDPI, Basel, Switzerland. This article is an open access article distributed under the terms and conditions of the Creative Commons Attribution (CC BY) license (<https://creativecommons.org/licenses/by/4.0/>).

1. Complexities in Fine-Grained Rocks: Some Terminology and History of Shales

The name *shale* /ʃeɪl/ dates back to the late 14th century, possibly as a specialized use of Middle English *schale* (“shell, husk, pod”; also “fish scale” [1]), or from Old English *scealu*, in its basic sense of “thing that divides or tends to separate”, from the way rock is broken into layers [2]. On the other hand, it could have come etymologically from the English dialect “shale dish”, used in the 18th century to name a black rock plate related to the British Mesolithic age, found on the Isle of Wight [3]. This area became known for the small discs of the same substance, named “Kimmeridge’s coal money”, and also supplied clays to make bracelets, amulets, or other decorations from the Romano-British period; the area is a bay and a small town in the Purbeck district of Dorset, southern England, whose rocky substratum makes up KCF (*Kimmeridge clay formation*), an important Upper Jurassic source rock in the North Sea [4].

The first technical use of *shale* appeared in The Miners Dictionary published in 1747 by Hooson [5], a term for a “clayey rock, laminated and hardened”, and was first recorded

in the 18th century to apply to a variety of fine-grained rocks [6]. Tourtelot [7] is a pioneer in the detailed review of the history of the terminology of such rocks.

In the literature, there are a plethora of names for these fine-grained sedimentary materials: lutites—*lutitas* (in Spanish, usual geological and engineering terms in Colombia, Peru, and Chile; also called *pelitas* in Argentina); siltstone—*limolitas*; mudstones—*lodolitas* or *fangolitas*; mudrocks—*rocas lodosas*; claystones or *arcillolitas*, and shales [8]. In particular, mudstone and shale have been the subject of debate, with well-dispersed literature [9]; their identification methods are ambiguous [6], which already implies difficulty in initial learning [10]. They have also been confused with other materials: for example, slate (*pizarra*, a metamorphic rock) was identified as being equivalent to shale until the 1920s [5]; a similar ambiguity persists today in Spanish with “*gas o roca de esquisto*”. The response to this is that the heterometry and structural variety, compositional complexity, and behavior from the micro-scale of such marine mudstones are, for Lazar and others, typically heterogeneous rocks [11]. *Shale* is still a snobbish, general and imprecise term [12].

Shale “is a sedimentary formation that contains gas and oil, whose defining characteristic is that it does not have sufficient permeability for these resources to be extracted with conventional methods”, according to YPF [2018: in [13]. However, it is indicated that “the term ‘oil-shale’ is actually a misnomer since the rocky unit does not contain oil, but soluble and insoluble chemical compounds, which can be distilled as hydrocarbons” [8]; the rock has terrigenous or chemical–biochemical constituents and carbonaceous residues (15%). Likewise, Yen and Chilingarian [1976: in [6]] noted that bituminous shale (oil shale) can be classified as tightly bound organic and inorganic “composites”.

Several authors prefer to use the name mudrock (as we have used it here) instead of shale to group all fine-grained siliciclastic, terrigenous, or detrital components, which may also contain biogenic components. For example, [14] divided the components into two classes: shales that have lamination or fissibility; and mudstones if they are not laminated. When they are lithified (or over-consolidated rocks, for geotechnical engineers), it is much more appropriate to call them “mudstones” since they generally mix mud with sand-sized sediments and organic matter (see Figure 1) in different percentages.

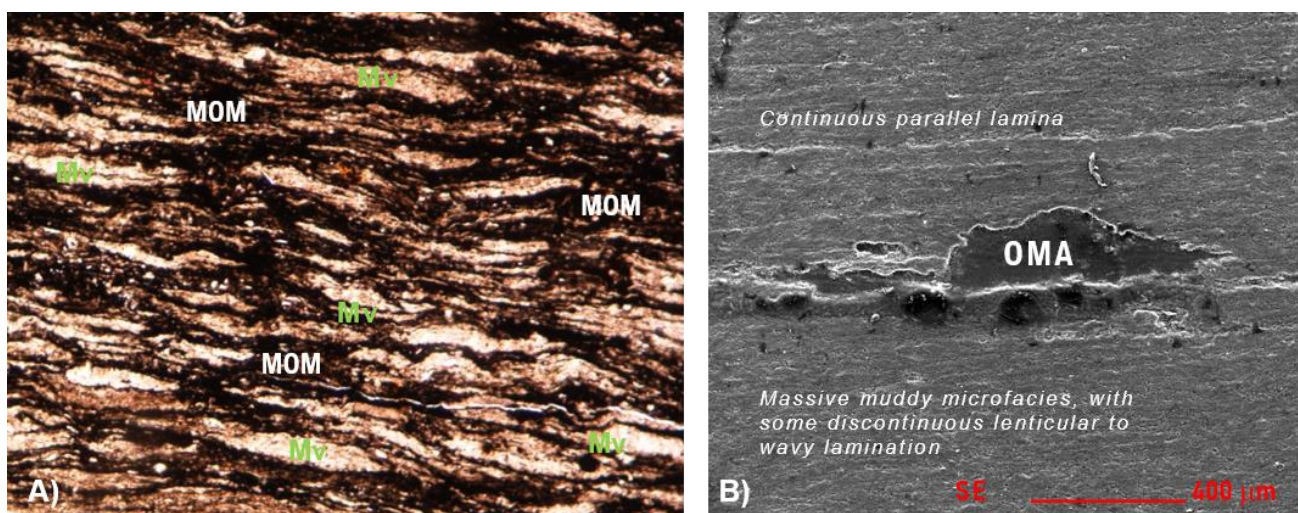


Figure 1. Granulometric complexity is identifiable only under the microscope (micro-scale level) in the mudstones of the Paja Formation. (A) 20X PPL petrographic microscope image: white flakes of muscovite (Mv) fine sand to silt sizes, which make up the fabric, and alternation of mats of microbiolytic organic matter (MOM, dark in the photomicrograph) with some fine light-colored siliciclasts that constitute the matrix: components are all oriented in wavy lenticular lamination. (B) an image of SEM secondary electron, SE, showing clay sediments (dominant size, so the rock is mud-supported) with organo-mineralogical aggregates (OMAs, sand size in the center). Note the submillimeter variation of lamination, identified instrumentally.

Firstly, there is the grain size, one of the twelve (and perhaps the most important) lithological textural elements. In this case, the sedimentary rocks have a muddy granulometry or “*lodo*” size, sediments with diameters less than 1/16 mm or 62 μm : the class is subdivided into silt—*limo* (term in Spanish) and clay grain sizes—*arcilla*, when the particles are smaller than 1/256 mm or 4 μm . However, mudstones usually also include the sand class (generally medium to very fine sand particles, with diameters between <0.5 and <0.125 mm), always in contents less than 25%, although for Dunham (1962), a mudstone has <10% grains (i.e., sands), all according to the classification scales established by Udden–Wentworth (1898, 1922) and Pettijohn–Potter–Siever (1987).

The second attribute is relative to the sedimentary structure: lamination (a lamina is a type of stratification that is less than 10 mm or 1 cm thick, above which the layers are), which is cited as always present in all shale. Lamination is caused by slight compositional variations from lamina to lamina [15]. Identifying the basic microstructure of clays (although not all particles are necessarily clay minerals), silts, and shales is fundamental to understanding the physical, chemical, and mechanical properties of fine-grained rocks [15,16].

On the other hand, fissibility is not a sedimentary structure or primary lithological feature per se, nor is it typical of such muddy rocks. “Parting” [17] is established as the property of a rock to divide along its sheets or layers, a tendency greatly enhanced by weathering.

This occurs in the mountains of Cundinamarca, Boyacá, and Santanderes (and also in Vélez), according to Figure 2. For them, the term fissile (or “*fisible*”, between 1 and 5 mm thick) indicates one of the five categories of parting [17]. Thus, in our opinion, fissibility is not a non-sedimentary property but rather a net product of exogenous geodynamics, specifically weathering [12,18,19], consistent with the researchers of [11,20].

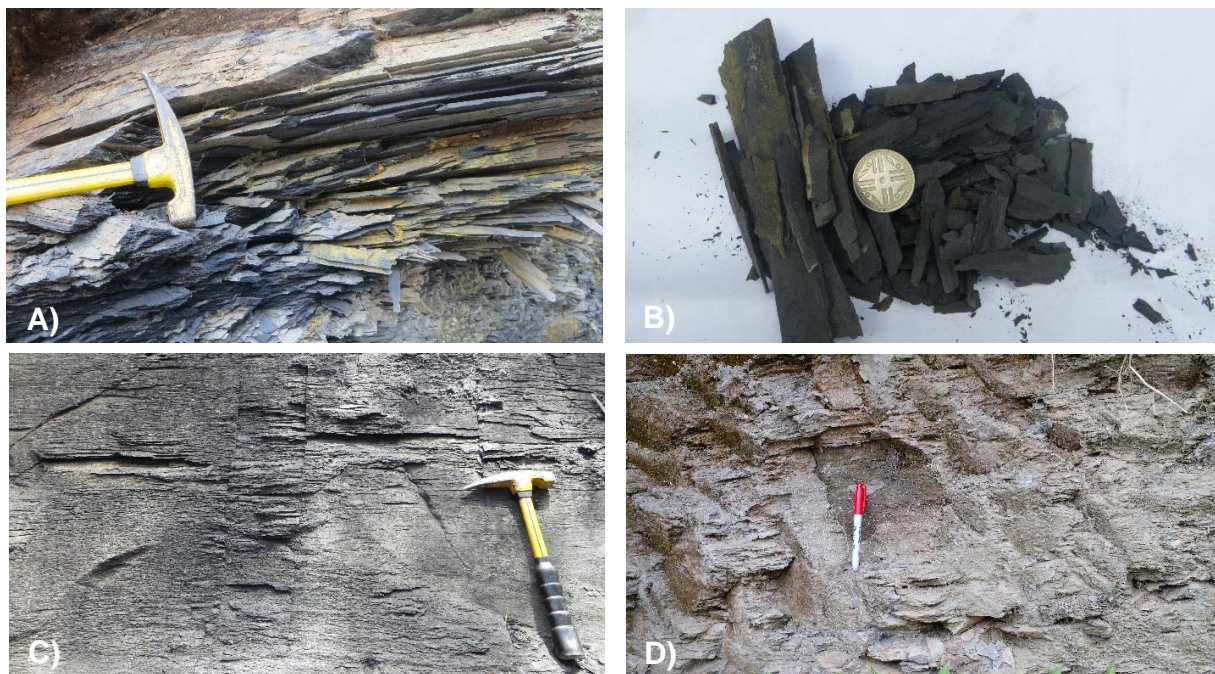


Figure 2. Outcrops and samples of mudstones in the Kip Unit, highlighting their structure, composition, and various colors (shades). (A) Straw strips or structures measuring $15 \times 2 \text{ cm}^2$ colored by weathering and its bituminous components (B), darker in color and smelling of sulfur; coin diameter 24.4 mm) on a slope in the San Luis neighborhood. (C) Massive to incipiently laminated rock with joints (vertical, closed); (D) observed in thick stratification and with discontinuous lamination, plane-parallel, in the outcrop of Palmira neighborhood, whose lilaceous color is due to the high content of pyrophyllite. Marker length = 12.5 cm.

Classifications based mainly on texture and structure have been proposed, such as in [17]. The shales and mudstones defined by fabric use alone are impractical as it does not consider quantitative compositional data [8]. Some even call them “organic mudstones” or “mature organic-rich marine mudstones” due to their origin and microbiological load [21], with which the composition is the third key attribute that determines them. The composition allows us to understand the history of the deposition, origin, and maturation of organic matter as well as the way in which both types of constituents interacted with pressure and heat [22]. Also, [9,15,23] suggest that the compositional properties of mudstones and shales should be used as modifying adjectives in basic textural names. However there are no easy answers, and no model is “one size fits all” [23], based on those considerations, classification systems, and nomenclature, as in [6,24,25]. Mudstones are inherently heterogeneous, composed of multiple component grains (a complex mixture of matrix minerals and kerogen) at variable proportions and a potentially wide range of properties; predicting key properties tends to be rather difficult [26,27].

Due to the foregoing, the objective of this work is to study the mudstones or “*lodolitas*” in their entirety; they not only offer mining and energy resources (i.g., iron, coal, uranium) and act as a geological seal for radioactive or toxic waste (of importance in aquifers and petroleum systems (oil and gas) and as raw material for construction, ceramics, and medical, cosmetic, and industrial uses) but also have other unfavorable attributes and behaviors. Additionally, we intend not to use the word “shale”, a famous industrial term in mining (as mentioned, within a kingdom that developed steam engines and imposed the use of coal for the industrial revolution between the 17th and 18th centuries), later used by the US military in the face of the serious instabilities of clay shale slopes [28] and globalized by the oil industry of the 20th century [29]. From technical advances generated by directional drilling, followed by hydraulic fracturing, shales are an exploration target: Barnett Shale was the first important work of what was originally called “*lutitas gasíferas*” (gas shales), an “unconventional” gas source [21], when George P. Mitchell combined both techniques for commercial production in 1998, starting point for geomechanics [30].

This is how the boom in the USA took place to extract hydrocarbons, beginning in the 21st century, especially oil shale, supplying national consumption and offsetting trade imbalances due to their dependence on imports [13]. Faced with a global energy shortage, the exploitation of shale gas greatly changed the pattern of natural gas supply; “oil-gas shales” was a widely used scientific term, statistically with high frequency, between 1998 and 2010 in China [16].

In addition to all these virtues, they also have a set of critical variables that can maximize negative processes in the face of human-natural triggers, as will be seen. In such a way, starting from such foundations, the general objective of this study is to characterize mudstones in relation to natural hazards, using multiscale methods and conventional and state-of-the-art analytical techniques.

2. The Vélez Case: Location and Background

The municipality of Vélez belongs to and is the center of a province of the same name, founded before Bogotá itself; It is a historical and commercial pole located in the southern part of the department of Santander, northeast of Colombia, South America (Figure 3A), and distributed on the Eastern Cordillera. This relief comes from the south in a northeasterly direction, arrives at the Santander department, and then turns northwest (Figure 3B). The town center is distributed on the hillside, on a step or step, long and with an irregular slope, with a concave trend and inclined towards the southwest, between 2030 and 2260 m above sea level. The studied area, local and specific, has 273.56 hectares.

There was an orthophotomosaic obtained by the Industrial University of Santander using UAV (eBee), generated and later restored with ArcMap in June 2014. The information was crossed with the urban cartography in the GeoDataBase format of the municipality of Vélez, delivered by the “Agustin Codazzi” Geographical Institute (IGAC). Other remote sensors (aerial photographs and satellite images) and DEM provided by the Government

of Santander and a shadow map with a resolution of 30 m were used. Thus, the basic cartography layers of Vélez were generated, with a level curve every 10 m.

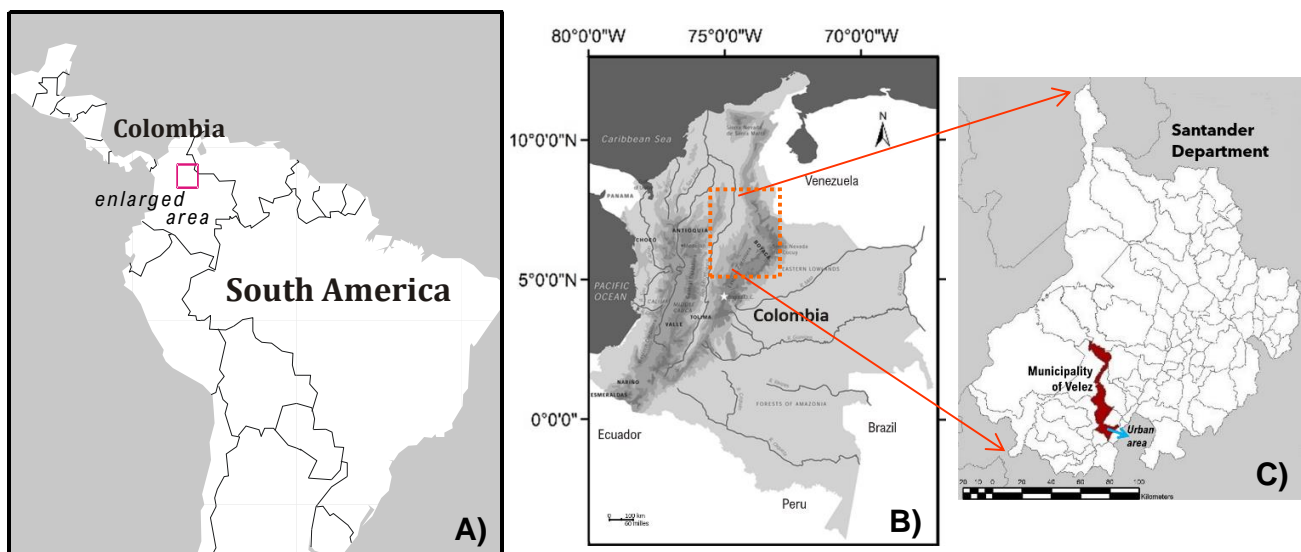


Figure 3. Continental (A) and national location of Santander in Colombia (B), and the municipality of Vélez (C), the urban area at the bottom.

Slope instabilities have affected the populated center of Alto Jordan since the 1980s, with damage to homes, schools, the Transversal del Carare highway, and the north of the urban area of Vélez, as well as the neighborhoods of San Luis, La Esperanza, Kennedy, and Ricaurte, with damage to homes and roadways [12]. The background to Vélez is given by previous studies and interventions by public entities at the tripartite level: with field visits by Ingeominas (from 1988 to 2011), the Ministry of Public Works and Invías, and territorial and academic entities. Additionally, thanks to a citizen, Veedora, and an environmental leader from Vélez, in the face of multiple landslides and dozens of affected households, in 2009, a legal action was filed to address the problem and identify risk mitigation measures. Consequently, inter-administrative agreements were made between the co-responsible entities, complying with the judicial ruling of the First Circuit Court of San Gil (in September 2011, ratified in June 2013 by the Administrative Court of Santander, who, in the same way, agreed with the managers of this popular action). The UIS is contracted with appropriate resources and, through the School of Civil Engineering and the Geomatics Research Group, has developed studies since the first quarter of 2014 with a group of senior specialists, professionals, and assistants in geology and engineering [31]. In the town of Vélez, several undergraduate theses in geology have also been carried out since 1994, including a master's degree in geotechnics, with attention given to these environmental impacts. Likewise, in order to reinforce the social appropriation of geoknowledge and risk mitigation, a book was published in 2017 [32], and various conferences, from the local to the national level, have been given [33–36].

3. Methods and Materials

The methodological scheme, sequence of activities, and levels of study are shown in Figure 4. Thus, for our multi-scale and nanoscientific characterization of the Paja Formation and its sedimentary deposits, secondary (preliminary activities and previous studies or basic cartography, shown in pink at the top of Figure 4) and primary information was articulated (combining field, laboratory, conventional, and nanoscientific data and office work, in addition to geomatic, geotechnical and geophysical surveys, environmental approaches, earth and soil sciences, and physical and chemical analyses), which allowed fully knowledge of the solid + liquid + gaseous components of both organic and inorganic origin, with

its spatial distribution generated by GIS. Also, the integrated characterization went from multi-proxy to upscaling: at the mesoscale, macro (topics of the central green rectangles in Figure 4), and cm–mm– μ m–nano levels, emphasized here, in order to understand part of the socio-environmental dynamics and their impacts on urban domains. Interaction of contributing factors gives rise to a complex geospheric system.

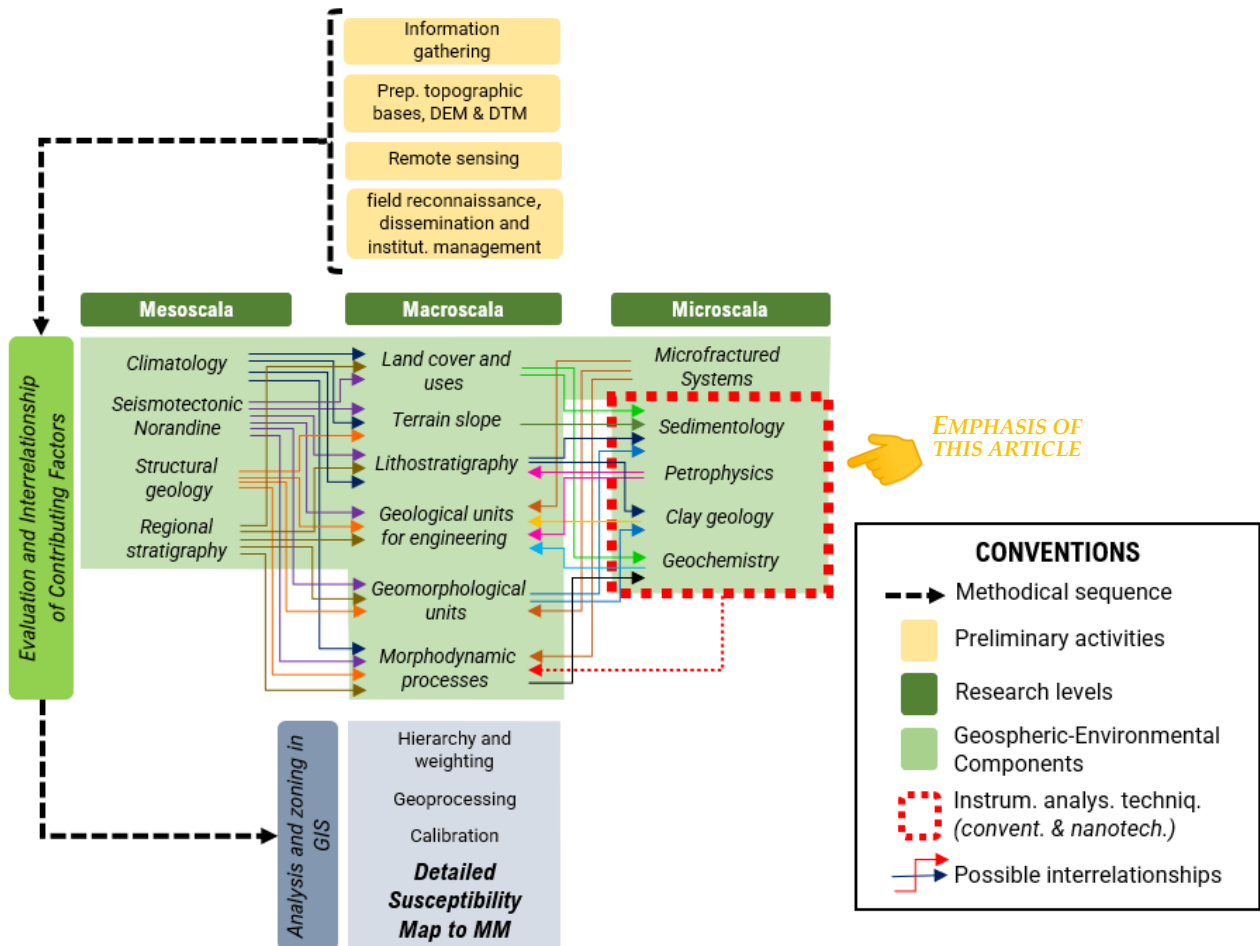


Figure 4. Methodological flowchart used in Reyes-Mendoza’s UB doctoral thesis (2019 version), with some of its products collected in this work. The phases, main activities, levels, thematic components, and analytical techniques (including microscale and nanosciences in the red dotted square on the right) are indicated in the central part. Contributing factors, from the subcontinental, national, regional levels to the local level, are inside the green rectangles; mapping scales (GIS analysis and zoning, below, in quadrangles of gray tones) range from a scale of 1:1,000,000, 1:100,000 to 1:2000.

The samples, investigated in detail, corresponded to mudstones, regoliths of the Paja Formation, and their associated colluviums, similar to sliding bodies and materials that integrate fillers, and are explored in slopes, cuts of roads, trails, excavations for houses, riverbanks or bottom-bases of a channel of a stream, or within paddocks of farms and plots of houses in the vicinity of the urban area and part of the central-eastern expansion zone of Vélez.

Fieldwork included georeferencing, column surveys and biolithostratigraphic correlations, and the sampling of fresh rock and weathering, regolith soils, fine colluvial matrices, and surface or groundwater in the urban domain of Vélez.

A preliminary visual inspection of the samples was carried out with magnifying glasses (manual and binocular lenses) and by means of a transmitted-light microscope. The nanoscientific techniques and equipment were: X-ray powder diffraction (XRPD), applied to rocks, soils and colluvium, in coarse fraction and with ethylene glycol solvation (thermal

treatment at 550 °C to identify expandable and interstratified minerals) using Bruker equipment D8 Advance running on Da Vinci geometry; a sequential X-ray fluorescence spectrometer with a dispersive wavelength of 4 KW (Bruker S8 Tiger brand), a scintillation and flux detector (for heavy and light elements), a rhodium tube X-ray source, and a high precision goniometer for theta angles and 2 theta; scanning electron microscopy (or SEM) with Quanta FEG 650; field emission gun electron microscopy/energy-dispersive X-ray spectroscopy (FEG-ESEM/EDS); SSD-type ETD and BSED detectors, performed in thin sections on fresh, weathered rock, colluvium samples, and nodules, with images taken in high vacuum and 25 kV accelerating voltage. For the detection of functional groups (from organic, non-crystalline phases), we use Fourier transform in infrared, with attenuated total reflection spectroscopy (FTIR-ATR), Nicolet is50 FT-IR equipment (Thermo Scientific), and an OMNIC program for spectral interpretation; a LabRAM HR Evolution Raman spectrometer; analysis of total organic carbon (TOC) and total sulfur (TS) by combustion in a high-temperature furnace with non-dispersive infrared detection (DNIR, LECO analyzer). Most of the mineralogical solid phases were determined through XRPD and the PDF-2 (2014) database of the International Center for Diffraction Data, combining the Edax Apollo X detector for semi-quantitative EDS (energy-dispersive spectroscopy) chemism in SEM with EDX Genesis software.

The Paja Formation mudstones were described in outcrop (96 geostations and control points in the field) as well as on both microscopic and nanoscopic research scales for the same sample using a Lupe, a stereo zoom microscope, a transmitted-light microscope (with seven thin sections, without and with coverslips), and the other instrumental analyses already mentioned (chemical analysis, 13 solid samples; 12 samples with XRD-FTIR; TOC-TS analysis, 9 samples), all to gain an understanding of what controls the type or distribution of petrophysical properties, and what environmental effects it has on locally identified geologic hazards. Regolith soils were also analyzed by the preparation of two thin sections for micromorphological analysis (with the help of the petrographic microscope). Therefore, in this work, we have integrated field evaluations with additional geotechnical and geophysical prospecting (core drilling and description, electrical resistivity tomography), which is not described in this manuscript.

4. A Colombian Andean Cordillera: Geological Framework and Physiographic Context

The Eastern Cordillera (EC), a young orogen (Cordilleran orogenic belts), separates the Orinoquia and Amazon basins from the Colombian Andean Block (CAB) continental growth by multiple accretion reaching [37], intracontinental [38] and wide plate margin deformation [39], and magmatism evolved in response to changes in the tectonic configuration [40,41], from transtensional/extensional conditions (215–145 Ma) to a transtensional regime (138–94 Ma), according to [40].

The northwestern corner of South America is a relict fragment of Gondwana [42], where interaction occurs between the South American continental plate and the Caribbean and Nazca oceanic plates [38,41], at which the CAB escapes to the northeast [43]. Mora's geodetic measurements indicate movement rates (GPS speed) of 16 mm/year, more specifically towards the north–northeast [2014: in [43]]. The department of Santander (Figure 3C) is representative of the confluence zone of these plates [44], next to the Chocó-Panamá indenter [45]. Chocó-Panamá block is the land bridge that connects Central and South America and forms the trailing edge of the Caribbean Large Igneous Province (CLIP) [46].

In Colombia, there are six natural regions, of which the Andean region (in the most central position) corresponds to the great mountainous belt of the Andes (divided into Western, Central, and Eastern Cordilleras, the latter separated by the valleys of the Cauca and Magdalena Rivers), according to [47]. The EC has the largest amplitudes or outcrop patterns from the Cretaceous, almost 170 km wide, from Cimitarra (Santander) to Aguazul (Casanare) [34], whose lithosequences are folded, faulted and uplifted, locally complete or subhorizontal.

Among its relief features, Cundiboyacense Altiplano and Sierra Nevada del Cocuy have the only snow-capped peaks of this mountain range (towards the eastern limit of the Boyacá department, on the southeastern limits of Santander; see previous Figure 3B,C).

5. Results

5.1. Lithological, Geochemical, and Petrophysical Aspects

With the integration of such tools, it was determined that the Kip unit has a sedimentary origin, terrigenous with their particular organic components, which were later lithified [19]: they are of marine origins with a bituminous component, with a strong mixture of crystals of siliciclastic contribution (represented by quartz, muscovite, a little microcline, and clays), typically aluminosilicates of K, Fe, Ti, Ca, and P (in crystalline and other amorphous phases) and organic compounds (called *rich-organic mudstones* here). They can be classified as *shale* (ar-fMs, Cs; ca-cMs, Zs), *clay-silty shale*, or *black shales*, according to the classification of Lazar et al. [11]. They are slightly sandy towards the top, with abundant kaolinite and pyrophyllite (up to 20%), zeolites, and high iron sulfides (framboidal primary pyrite $\leq 7.8 \mu\text{m}$, cubic pyrite, siderite and amorphous authigenic marcasite with tens of microns), with inorganic phosphates, sulfates, iron oxyhydroxide (goethite, lepidocrocite), and heavy minerals (titanite, anatase, zircon, etc.).

Organic matter occurs in various forms or contents and is discrete, micro-biolytic (MOM), laminated, and in intraclasts or organo-mineralogical aggregates (OMAs). There are submillimeter fragments to micro-mats of *phaeophyta* and occasional gyrogonites of *charophytes*, typical *ammonoids* in thin calcareous or replaced casts and mono-order, no larger than 5 cm. Predominant lithological features (macro- to micro-scale) of the Kip unit are shown in Figure 5.

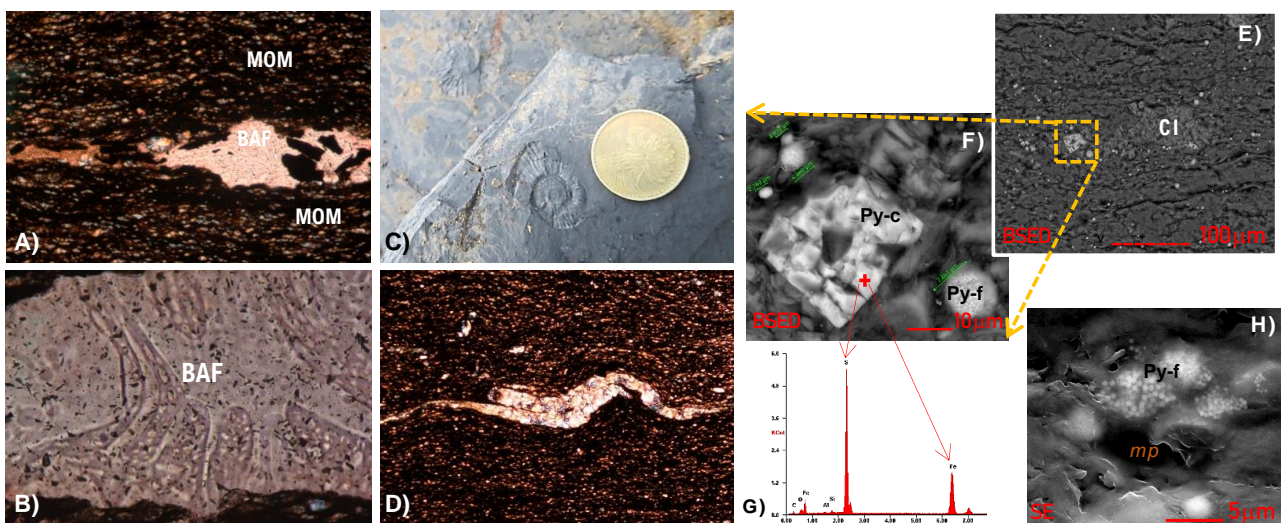


Figure 5. Details of texture, structure, composition, and fossils in the mudstones of the Paja Formation. (A) A 1.3 mm brown algae fragment (BAF) seen in thin section, within microbiolytic organic matter (MOM) and phyllosilicates, silt and clay sizes: corroded and partially replaced by CaCO_3 , pyrite, and siderite at the edges red wine color (magnified 10 \times); (B) with ellipsoidal zoetia and elongated avicularia, zircons, and other accessory minerals (40 \times , also in XPL). (C) Ammonites: above, in molds in the gray mudstone (coin diameter 20.3 mm); (D) double shell (max. thickness 20 microns, in 5 \times XPL) in high carbonate birefringence colors. On the right, SEM of another claystone with iron sulfides and a few layers of MOM: (E) compacted intraclast (CI) with pyrite of cubic (Py-c) and framboidal (Py-f) habits, enlarged in (F); the + locates the punctual EDS (G), with S and Fe spectrum, iron sulfide. (H) intergranular microporosity (mp) in “fresh” rock, and unaltered iron sulfides.

Additionally, locally, there are agglutinated benthic foraminifera (possibly abyssal), calcareous filaments, and bony micro-remains (spines, vertebrae) in the lower and middle part

of the sequence. The other phyllosilicates (hydroxides and oxides of Al, Si, Mg, Fe, etc.) are: dickite (13%), illite (11%), gibbsite (5%), berlinite (9%)/nacrite (3%)/chamosite/clinocllore, halloysite, and vermiculite [18]. The crystalline phases reach a range between 55% and 69% [12], although the rock also has a rich biogenic signature, with TOC > 5 and TS 4.8%, towards the easternmost urban part. These sediments are considered non-calcareous (Ca < 4.3%), with dolomite–ankerite in fine euhedral crystals, very subordinate calcite, and some top layers with siderite nodules–lenses [19].

Algal mats and ammonite fossils suggest a possible “algal bloom”, which, together with framboid pyrite, iron minerals, and local micro-concentrations of heavy metals and rare earths, are indicators of toxic environments and consistent with a strongly anoxic oceanic environment [18,19]. On the other hand, in the IR analyses generated by ThermoFisher Scientific Inc and the spectral interpretation of bands, the following functional groups were found, in order of importance: inorganic phosphates, aliphatic primary amines, aliphatic primary amides, nitro compounds, and aliphatics and aliphatic hydrocarbons. Such amines are products of the biogenic decomposition of algae + plankton, being consistent with what was previously expressed.

In terms of structure, they are predominantly massive mudstones (the samples exhibit a tight texture), with solid nodules and pyrite holes [19]. At the micro level, they show wavy and lenticular lamination, not parallel and always discontinuous, very locally flat-parallel. The fissibility of the rock is not conditioned exclusively to the presence of clay minerals and micas but to the sets of discontinuous laminae, with interconnected algae and MOM “tapestry” (Figure 2A,B), together with the AOM and CI.

All these fabric and compositional aspects allowed the biostratigraphical subdivision of the Paja Formation into four segments: Kip1, Kip2, Kip3, and Kip4. Regarding the Quaternary deposits, sedimentological characterization and morphological position allowed the mapping of eight colluvial deposits, somewhat scattered and with maximum thicknesses of 2 m, along with the narrow recent alluviums associated with the Las Flores, Puente Los Rios, Palenque, and Las Lajitas streams, which flow from west to east inside Vélez, within very youthful valleys.

Various porosity types are recognized: organopores, intraparticle and interparticle pores, and some microfractures. Important primary microporosity was identified and quantified in max. 8%: it is intragranular (within the thicker components or the framework, whether terrigenous, biological, or diagenetic minerals), intercrystalline (in micas, clay minerals, etc.), and intergranular (between matrix and framework).

Secondary porosity is higher and associated with structural discontinuities such as stratification, lamination, joints, irregular fracturing systems, and regional foliation features in the rock. This was not investigated per se, but there is evidence of So plans due to burial and possible foliation S1 [12]: thus, these mudstones are already metapelites (with low-grade metamorphism; perhaps epizonal?), corresponding to the high pyrophyllite values found (max. 20%).

The microporosity is of the honey, cubic, or amorphous type (related to the dissolution of iron sulfides, barium, carbonates, and tectosilicates), which, together with permeability, increases due to the weathering processes (oxidation/dissolution/hydrolysis) acting on the fresh rock. Depending on the specific lithology and geochemistry (Figure 6), with its facial changes, there is spatial variation in susceptibility to the geological processes now cited.

This facilitates the chemical dispersion and mobility of fluids within the rock mass, deepening (observable to average levels not greater than 1.2 m) and making it more friable, especially in the horizons or faces closest to the surface [18], as is evident in roads, escarpments, or urban excavations for housing, roads, facilities, or other infrastructure.

The role of hydrobiogeochemical reactivity is explained at the end of this article since it is in direct interrelation with other relevant exogenous phenomenologies.

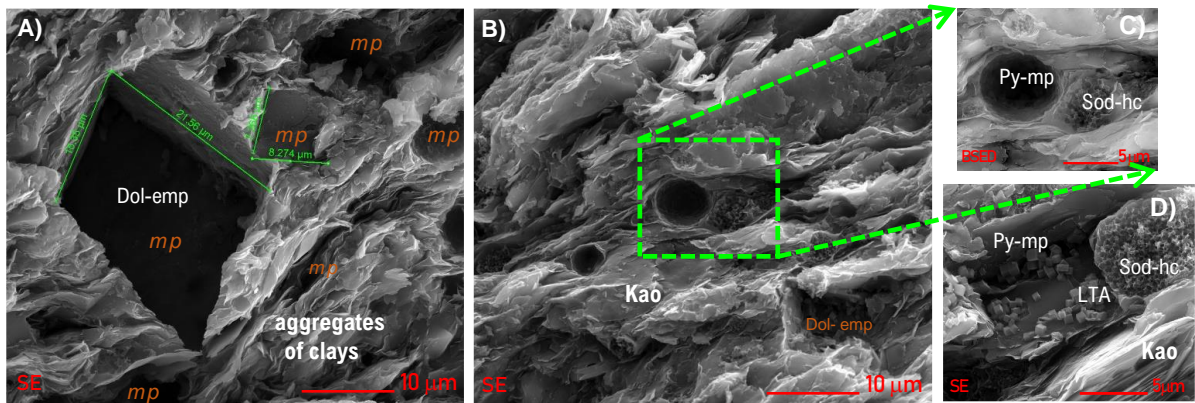


Figure 6. High-resolution SEM photographs showing typical petrophysical properties in materials from the Paja Formation. (A) Rock with a clayey matrix (aggregates of clays of kaolinite-type in curly lamellae) and euhedral moldic pores of dolomite (rhombohedra, with faces between 8.2 and 21.5 μm). (B) Micropores by various framboid pyrites and carbonate, towards the bottom, in a regolith sample (poorly developed soil, but with higher secondary porosity than fresh rock), which is magnified in (C): micropores of honeycomb sodalite and an orbicular cast left by iron sulfide (6 μm diameter) between kaolinite booklets. (D) Another aspect of weathered mudstone: phyllosilicate minerals beside the poral aggregates of sodalite and pyrite are shown (interconnected microporosity), in whose cubic mold’s zeolite Na-A crystallized in stacks of “sugar cubes”, a fact reported for the first time naturally. Microporosity is symbolized in photomicrographs as mp; emp: euhedral moldic pores; hc: honeycomb; Kao: kaolinite; Dol: dolomite; Py: pyrite; LTA: Na–A zeolite; Sod: sodalite.

5.2. Weathering and Hydrogeochemical Reactivity

Weathering clays are dickite, illite, gibbsite, halloysite, and kaolinite (<4%), which, with various zeolites, give variegated colors in colluvium and regolith (Figure 7).

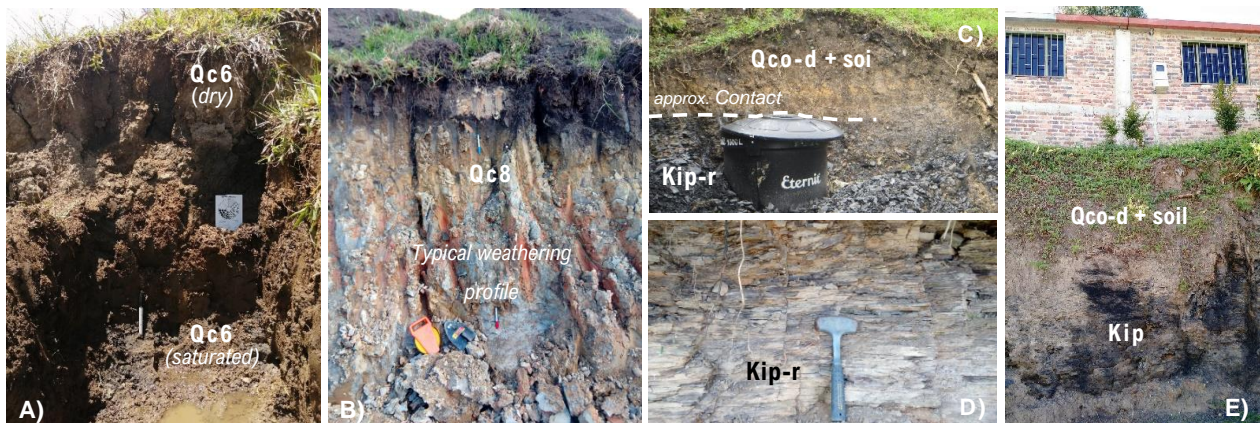


Figure 7. Field occurrence of the materials (surface formations) covering the rocks. (A) Unstable sandy–muddy colluvium in a paddock uphill from América India neighborhood, in whose trench a sample was taken for soil micromorphology. (B) Another colluvium of silt–clay matrix, typically variegated by the presence of oxides, hydroxides, clays, tectosilicates, zeolites, or other crystalline and organic phases, deeper and developed on a flat morphology zone (around the La Rosita neighborhood, east of Vélez) and with high recharge. (C) Weathered mudstone (dark gray), in transitional contact with a mixture of soil and dispersed (-d) colluvial material, of brown, yellowish, and gray colors, with angular lithics, in the back garden of a Palenque house. (D) Outcrop in the village Las Amarillas, whose petrophysical properties have increased, being more friable and susceptible to mass movements. (E) A house in Ricarte neighborhood founded on residual soil mixed with discordant colluvium on the marine rocks (masked by clear patinas of weathering). Q: Quaternary; c: colluvium; Kip-r: regolith of the Paja Fm., dated to the last period (Ki) of the Mesozoic era.

They are light gray, yellowish, and brown to reddish in color [34,35] to purplish-bluish (when it is dry and pyrophyllite abounds, as in Figure 2D). It should be mentioned that the zeolites have very significant contents, and it should be noted that sodalite is associated with zeolite Na–A or LTA, which is reported naturally worldwide for the first time and, for now, exclusively within the Paja Formation [48]: it shows high concentrations of Al (17.97 wt%), Si (27.14 wt%), and O (9.63 wt%). The soils mixed with colluvium, which contains the highest concentrations of zeolites (vermiculite up to 3.5%, ZeoSSZ, ZeoX, ZeoY, fausajite, garronite), are just below the old houses of the town of Vélez, characterized by their clay granulometry, high plasticity, and homogeneous yellowish to beige colors, up to 2.5 m thick.

In accordance with the petrophysical susceptibility of the rock, the anisotropy is of the 3D type: the “degradation orchestra” leads to uninterrupted processes of oxidation of sulfides, sulfates, metal oxides, and hydroxides, the dissolution of salts and silicates, and the leaching of the few carbonates, with neoformation of the aforementioned clay minerals. It was determined that the organic compounds help wash the regoliths and colluvium, reaching almost zero concentrations of C (0.3%), Ca (0.08%), and S (0.004%). Ferric oxide increases by weathering up to $\geq 11\%$, along with the pH; additionally, anatase contents indicate strong chemical weathering [18]. In the colluvions of drier areas, SiO₂ is preserved (57–52%), along with Al₂O₃ (28–22%), CaO (0.76–0.53%) and TiO₂ (1.1–0.9%), indicating less washing of minerals and the presence of Fe oxides with respect to the western urban slope (potrized, high and humid; [34]), which has comparatively low SiO₂ contents (48–46%), TiO₂ (0.8%) and especially CaO (0.11%), leading to a slight increase in Al₂O₃ (29%).

In particular, physical and chemical weathering thus generates very plastic regoliths under the old houses of Vélez (in the historical center itself, some with more than 350 years of construction) that have beige-orange colors and are >2.2 m thick, insulated by hard surfaces; they are almost non-existent on the western urban slopes, overlying or mixed with unstable colluvial deposits [19].

It is established that the hydrogeochemical dynamics is regulated by: hydroclimatic and environmental conditions of the urban area studied in the regional context (precipitation regimes, natural humidity in the soil and air, the volume–depth–direction of surface water currents, and the hydrogeological flow, which are oriented negatively towards the urban area from the highest western slopes, which are quite pastured or have fragmented forests). The geospheric component is rich in sulfurous minerals (pyrite, siderite, see Figure 5A,E,F,G, marcasite or barite), typical throughout the Kip column, which, when weathered (chemical reaction air + water + rock that contains them), creates sulfuric acid H₂SO₄. It is one of the strongest mineral acids, known as acid mine drainage or AMD.

This poses a health challenge, given that Vélez has not resolved the supply of drinking water: in neighborhoods such as La Esperanza, about a dozen wells and artisanal cisterns exploit groundwater levels, domestically and even commercially. AMD also prevents plant growth due to the successive accumulation of Fe and S, which makes root penetration difficult. The tendency of the runoff flow towards the urban area originates runoff (of hard water, rich in sulfates and dissolved heavy metals), contaminating subsurface waters or downstream catchments and the infiltration and recharge of local–subregional aquifers. Flow paths (interflow or shallow slope flow vs. deeper groundwater flow and its mixtures) respond to secondary permeability related to weathering but adversely intervene in the outflow from the basin at depth.

The penetration of the first oxygenated interflow under the valley sectors leads to more oxidation of pyrite–marcasite, iron oxides and oxyhydroxides, and alumino-silicate hydroxides, releasing more sulfuric acid and weakening the rock masses “in crescendo”, that is, giving greater hydrogeochemical reactivity to the four segments of the lithological unit. In turn, the cascade of reactions proceeds, which produces more regoliths and breaks down the colluvium matrices. Such hydrogeomorphological processes have already been evidenced by various authors in analogous basins with bituminous mudstones rich in pyrite, for example [49,50].

The basic water analyses, obtained at the sites and points shown below, indicate the following: the surface waters in the El Palenque and Las Flores streams (Figure 8A,B) have the highest pH, 8.33 and 8.20 units, respectively. On the contrary, the water in the domiciliary cisterns (Figure 8C) has a lower pH (6.89) but with the highest concentrations of total alkalinity (158.19 mg CaCO₃/L), sulfides (185.5 mg S⁻²/L), carbon dioxide (42.71 mg CO₂/L), and bicarbonates (96.59 mg H₂CO₃⁻/L). Total alkalinity (127.92 to 146.48) and bicarbonates (78.83 to 89.85) are slightly lower in those runoffs, with very low carbon dioxide (1.28 and 1.465). Likewise, the waters that come out of the geotechnical drains (Figure 8D) to the urban south and within the mudstones are rich in gypsum and have a pH of 6.77, the lowest contents of alkalinity (105.46 mg CaCO₃/L), and bicarbonate (63.4 H₂CO₃⁻/L) values of 182.5 mg S⁻²/L and 40.07 mg CO₂/L. Both subsurface waters are considered acidic, corrosive, and soft, with metal ions that can be toxic: iron, lead, manganese, and zinc.



Figure 8. Points where water samples were collected: (A) in the El Palenque catchment; (B) Las Flores drainage (behind the houses), on the road to Las Amarillas village; (C) at the bottom of the drain on the national road, south of the study area, with reddish patinas due to oxidized iron sulfides; (D) in a cistern inside a house, La Esperanza neighborhood.

Likewise, the mixture between the gypsum and these waters generates a heat release reaction, which is called an exothermic reaction. This theoretical condition was noted in the outcrops, with gypsum (in millimetric, colorless, and translucent sticks) finely laminated in the black mudstone, as found between the Santa Teresita and Antonio Ricaurte neighborhoods, just where a groundwater line emerges: removing and palpating a rock sample has the sensation of moisture and being somewhat warm, and it is much more friable in the hand than the rest of the materials analyzed in the urban area.

There are more concentration and perennial flows of groundwater, brought down by multiple sub-horizontal drains built by the INVIAS on the entire western margin of the national highway—they have the particularity in their flow of staining slopes, ditches, or sewers with reddish-brown color due to the AMD of the pyrite microparticles.

The gypsum facies mapped on the detailed geological map (edited at a scale of 1:2000) coincides with the subsidence zone identified and inventoried in the south of the urban area [18,35], concentrating the waters already described. In addition, the heat due to exothermic reactions has a possible connection with the manifestations of spontaneous ignition in the rural areas of Vélez.

5.3. Rare Earth Elements (REEs) and Their Associations

Several heavy elements (HE: Ti, Pb, etc.) were identified with qualitative instrumental techniques, including silicates with rare earth elements, mainly from the lanthanoids group. Total RREs content is strongly bound to inorganic matter. When RREs occur, they light up and stand out easily in SEM electron beams. Figure 9 shows the SEM images of weathered muddy rock samples, with the solid substances that were determined by EDS point composition (Figure 9B–D, in both extremes): in sparkles inside the massive lodolite (Figure 9A), Pb 70.12 wt%. Solid materials provide favorable ore storage and punctual

space for mudstone-type mineralization that has particular mineralogical habits: e.g., the REEs are botryoidal clusters smaller than 5 μm , according to Figure 9C; Ce (4.08 wt%), La (1.75 wt%), Nd (1.25 wt%), and Sm (0.53 wt%). A silicate mixed with phosphorus, 10.55 wt% (Variscite, Berlinite minerals?) + OM (11.57 wt%) houses it.

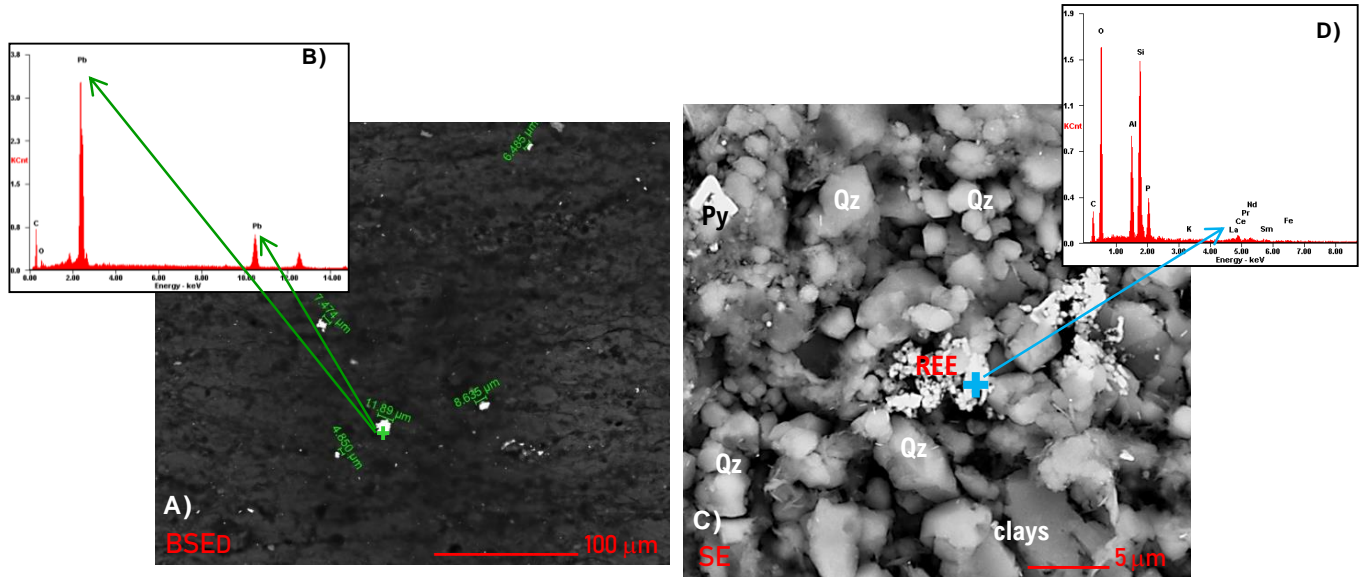


Figure 9. Detail of metals (A) and rare earths (C), identified by SEM within the Paja Formation, that accompany siliciclastic minerals, clays and others; at the extremes, the EDS spectra (B,D). (A) backscatter micrograph showing lead particles from 4.8 to 11.8 μm in particle diameter; (C) SEM secondary electron image of a fine silt and clay (top 3.9 μm , bottom) sized sediments, with quartz (Qz), iron sulfide (Py), REEs (see microanalysis report in text), and aluminosilicates (elements in the peaks, left, of the respective spectrum, (D), plus C and P. Note some scattered halloysite nanotubes.

Too, a 4.5 μm hexagonal phosphate (P: 11.57 wt%) was identified, very bright in BSED due to REEs. EDS microanalysis determined, in wt%: Y 24.67, Dy 4.23, Er 2.21, Gd 1.76, and Ho 0.59). So, it is the mineral Monazite-(La), formula LaPO_4 .

The increase in ERR concentrations is due to silicon and aluminum oxides (aluminosilicates), and they have bound elemental associations and with some minerals: Titanium (Anatase, Titanite, Rutile, Titanomagnetite); Cesium (light alkaline, a constituent of complex minerals: reacts vigorously with oxygen to form a mixture of oxides; in moist air, the heat of oxidation may be sufficient to melt and ignite the metal, given its low melting point and violent reactivity with water, which could be considered in Section 5.5); Rubidium (with which Cesium has a strong chemical association: Lepidolite, mica group, contains up to 3.5% rubidium); and Lepidocrocite (a common mineral hydroxide in deposits with abundant pyrite). Geochemical characteristics of REE and their geological significance in the mudstones of the Kip are beyond the scope of this work, although organic fractions in this rock classes have been used to investigate the reliability of REEs as a tool for oil-source correlation [51].

5.4. Geomorphological Processes

In the Vélez urban area, different mass movements (MMs, or mass wasting) were observed, characterized, and inventoried at a 1:2000 scale, including the multi-temporal monitoring of the largest movement, using remote sensors (Figure 10). In order of importance, the types of MM are: *translational landslides* (with laminar geometry and always <1.5 m deep: [12,33,34]), involving regoliths or incipient soil profiles, material from the different translocated deposits (from the rock–colluvium interface), which are evident in contiguous colluvial rural areas; *wedge slides* (controlled by bedding and weathered and

heavily jointed rocks); *block slides* (at massive levels, fractured and following the dip); *flows* (mud, debris, and creep); and *rock falls* [32].



Figure 10. Mass movements present in the jurisdiction of the municipality of Vélez: (A) Earth flow seen in the Troncal del Carare road corridor, which started as translational type and in paddock grounds; (B) laminar landslide just to the west of the study area (seen in the background, on the Palenque ravine), which laminarly mobilized the regolith at the end of August 2020; (C) debris wedge slide on the road cut slope between Aquileo Parra and Kennedy neighborhoods (activated in October 2016). (D) Removal caused by excavations for a shopping center in the Las Nieves neighborhood, which affected 3 houses and forced the suspension of the project (February 2017); it exposed a thick and ancient soil profile that had zeolites and abundant alteration clays.

In the municipality of Vélez, creep is the most extensive process, and although it's having a very low kinematic rate of displacement (of a few mm or microns, geotechnically modeled with the Plaxis program), they induce deformation and serious cracks in constructions, such as in floors and walls of houses. These problems gave rise to the popular legal action already mentioned, established at the courts of San Gil.

There are also important manifestations of *subsidence* [12,18], which is not really a slope process but an MM that has a net displacement only in the vertical component. In addition, the area to be inventoried in the field and mapped geomorphologically was evaluated using sedimentology, petrography, and nanotechnology.

Thus, a broad *gypsum facies* was recognized [18,19] as the direct cause of local MM problems (see Figure 11): the gypsum is a calcium sulfate dihydrate, which, here, has a militabular, fibrous, and irregular habit, finely interlaminated within the bituminous mudstone (Figure 11C–H); its low relative hardness and/or high brittleness can cause the mineral to collapse within the rock, under static or dynamic loads, without considering all the shallow to subsurface hydrogeochemical activity [19,34]. The samples analyzed are usually accompanied by barite, salts, MOM, etc.

This process, which was detected by the Reyes-Mendoza doctoral thesis and not in the 2015 UIS studies, was towards the base of the entire muddy sequence. It occurs to the south of the urban area, on the national paved access road from Barbosa, which continues towards Cimitarra, also involving the old Calle Real, roads that correspond to the third and second streets in the urban nomenclature (see the photos in Figure 11A,B), as well as in the adjacent sports area of the Ricaurte neighborhood and the Sanandresito settlement.

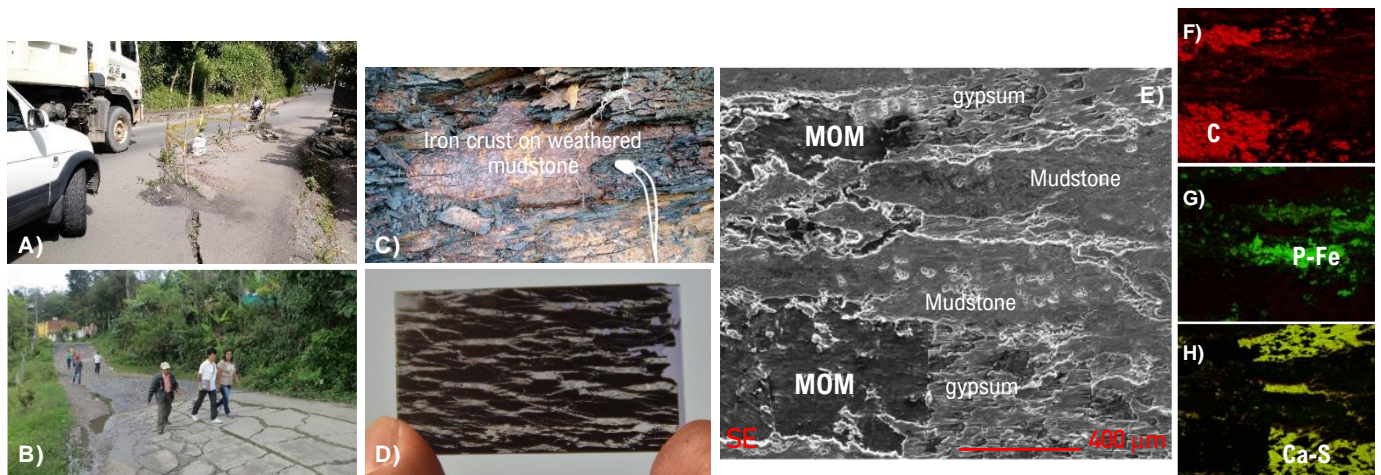


Figure 11. Subsidence in the national highway (A) and deformation in the old Calle Real (B) access to Vélez due to the presence of gypsum. Outcrop (C) where the stratigraphic column was lifted and samples were extracted for laboratory. Thin section ((D): $4.5 \times 2.7 \text{ cm}^2$) showing the fibrous and colorless gypsum in sheets, anastomosed within the gray mudstone. SEM-SE image (E) of the morphology of the components in thin section, subjected to EDS compositional mapping, in distinctive colors: (F) red, carbon (C) or organic matter corresponding to the dark sectors in the micrograph; (G) green, phosphorus (P) plus iron (Fe); (H) yellow for calcium (Ca) beside sulfur (S).

Although it is a local phenomenon, it is very dangerous for the people, housing, and civil infrastructure there; this problem has a great negative socio-economic impact due to the fact that it recurrently interrupts vehicular traffic.

5.5. Spontaneous Ignition

As has been observed by the authors in Kip mudstones (muddy marine and bituminous rocks), spontaneous combustion is a common phenomenon in the Eastern Cordillera: in various areas of Santander, the municipalities of Simacota (Santa Ana del Olvido town) and Oiba, and the villages of Las Amarillas and Loma Alta de Vélez. In Figure 12, such materials, characteristics, and phenomena can be observed, including the field visits and technical reports of Castro [52,53].

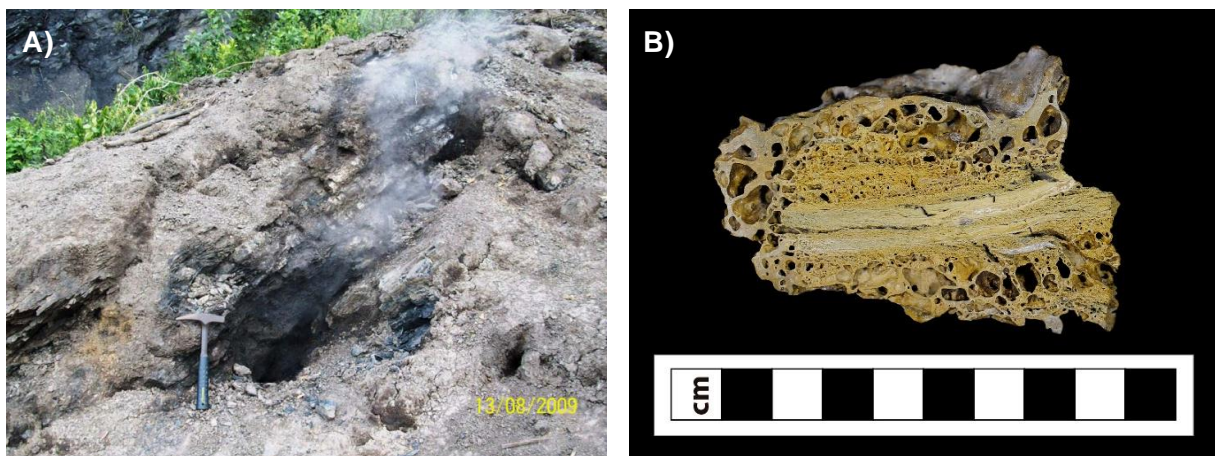


Figure 12. Photographic record of spontaneous ignition (A) due to low-temperature oxidation in Kip mudstone from Loma Alta, emitting toxic gases; (B) charred hand sample (clinker), with very high porosity and permeability generated by the combustion and pyrolysis processes of hydrogen sulfide and macerals within the rock.

During fieldwork carried out in August 2009 at the Guayabal site in the Loma Alta village, a sequence of photographs documenting the phenomena and relevant inhabitant testimonies were collected. Castro's report [52] mentions: "the landslide began approximately a year ago during the rainy season, but in the last 45 days, it was reactivated for the same reasons and began to generate heat and gas emissions that became larger when it rains". The source of the heat is located within the slide mass and is due to the fact that the rocks have high contents of organic matter; the combustion is similar to that generated by poor quality coal when it burns, releasing heat and giving off gases and volatiles such as carbon monoxide and sulfur, which cause health problems [52].

Elsewhere, researchers have said that they "burn with a bright flame, giving off considerable heat and an unpleasant odor" due to the combined geochemical processes of combustion and pyrolysis [50], which can be accelerated naturally and/or anthropically. The combustion of mudstone has been reported at times in outcrop deposits and mining piles; the particle size is a critical control of auto-combustion [54]. Additionally, [55] shows that the oil shale generates gaseous products, such as CO, CO₂, CH₄, C₂H₄, and H₂, which might be due to the oxidative decomposition of aliphatic hydrocarbon and the oxygen functional group: with the increase of temperature, the contents of CH₂ increase, whereas those of C–O increase first and then decrease; the smaller particle size has a lower critical temperature and, thus, consequently increases the susceptibility of samples to spontaneous combustion. This is analogous to what was observed by the authors of [54], who indicated that shale is reactive and highly dependent on particle diameter and that the self-ignition of small particles is possible in outcrops exposed to oxygen for deposits of thicknesses between 10.7 and 607 m at ambient temperatures between –20 and 44 °C. The characteristics and mechanism of spontaneous combustion provide a theoretical basis for preventing the spontaneous combustion of oil shale [56].

In the case of Vélez, the direct or real cause of such ignitions, namely, auto-combustion and what can also be categorized as underground fires, is the direct decomposition of algae and other discrete or microbiolytic organic matter that create an environment loaded with hydrogen sulfide (H₂S); this is undesirable for the locals, as well as being unhealthy for others. It was noteworthy during the acquisition of images with SEM for samples in thin sections (without coverslips, placed on metal stubs with adhesive carbon tape) that applying a graphite coating on the Quorum 150ES equipment helped to avoid the dispersion of electrons; in the sectors with a greater presence of organic matter, its functional groups are good conductors of heat and generate millimeter-sized "blisters" in the thin section, just above the sector where the electron beam from the environmental scanning equipment hits (using Schottky field emission gun technology). It is quite possible, due to the stimulation of hydrogen sulfide, that a gas that is sensitive to temperature has flammable behavior.

6. Discussion

Mudstones and mudrocks, although at first sight, appearing monotonous, are actually micro-heterogeneous and very difficult to study, even under the microscope. For this reason, we address them in their entirety, combining nanosciences [57], classical techniques, and new proxies for quantitative characterization [26,27,58].

For the authors of [8,9], sedimentary texture encompasses three fundamental properties of sedimentary rocks: grain size, grain shape (mentioned just starting), grain shape (form, roundness + sphericity, and surface texture or microrelief of grains), and fabric (grain packing and orientation, arrangement frame). Grain size and shape are the properties of individual grains, while fabric is a property of grain aggregates [8] that are larger or more abundant within the rock. In sedimentology, pore space and permeability are considered textural elements too [34]; as the texture becomes finer or as silt plus clay increases, total pore space increases, together with the range and diversity of pre-sizes and shapes [59]. Pore connectivity is one of the most important characteristics of shale reservoirs because it significantly impacts the effective pore space, permeability or fluid migration [58], and

water accessibility [60]. The pore microstructure of fine-grained sediments is highly dependent upon the scale at which it is considered [27,61] and porosity also varies over more than an order of magnitude in spatially continuous mudstone layers, being consistent with [62]. According to Slatt et al. [63] porosity is less when measurements are made on surfaces parallel to laminations, than on surfaces perpendicular to them, owing to the platy nature of the contained clay minerals; proportions of micropores (defined as $>1 \mu\text{m}$ in length) and nanopores ($<1 \mu\text{m}$ in length) are about equal in different shales, appreciations that we share. Its variations go in the 3 dimensions.

Due to weathering, in an environment observed for several years (2014 to 2021), specific microsurfaces are generated, in a degradational continuum system, in the most superficial mass rock, considered by many to be true 'aquifers', within a high flow mechanics. Hydroclastism (a type of physical weathering in muddy rocks) mechanically produces milli- to micro-partitions by successive cycles of wetting and drying (expansion vs. contraction, volumetric changes and particulate disintegration), depending on the weather (water, wind, variations of heat and cold, dry-humid, that produce drastic drying and wetting stages in the rock, with direct effects on slenderness), and hydroclimatological-biotic variability and the use of urban or rural land. Chemical weathering controls the composition of the rock in terms of kinematics, intensity and duration of surface changes, of the solid, liquid and gas phases; in particular, the oxidative dissolution of abundant iron sulfides (cubic, framboidal, amorphous pyrite; irregular siderite and marcasite), oxides-hydroxides, carbonates (calcite, dolomite), silica and sulfate in solution, Fe and Al or Li phosphates, ions and salts (for example, Na and K are soft, chemically active, alkaline metals that make contact with nonmetals, easily forming salts), sodalite (rich in sodium and other metals) and other silicates, hydrates, dynamically generated modified in these environments, without considering other crystalline or organic phases, as analyzed in Section 5.2, generating micro and nanopores. The primary microstructures, joint systems, or geological faults increase the mobility of fluids, also helping to generate new and numerous specific, highly reactive, and unstable microsurfaces. All these components are destroyed and create a new secondary microporosity and permeability, increasing the transmissivity (fluid flow), allowing the geochemistry remobilization and/or recrystallization of pre-existing silica, zeolites, kaolinite minerals, salts, oxides, and peroxides [48], with which the geomorphological susceptibility of the terrain grows [34,36].

These substances undergo further oxidation and chemical dispersion (with sedimentation-suspension in sufficiently large particles or as colloids and solutions for the smallest ones). The products are also mixed with more acids, e.g., carbonic acid (a weak but abundant and corrosive acid), humic, tannic (interrelated to organic, climatic, or human conditions), or other loads in sewage and urban discharges. Although they are not monitored physico-chemically or bacteriologically, these processes require contributions from environmental and sanitary engineering. Here, are required contributions from environmental and sanitary engineering: more integrated studies to monitor, characterize, quantify (physiochemically or bacteriologically), model and assess the relative importance of these hydrobiogeochemical processes, small in scale but very incessant. Some analogous interpretations are those of [49,64,65].

However, the most dangerous is AMD, which is very corrosive and water-soluble. In highly anthropized areas, the mechanization of the soil and the increase in excavations for road corridors, aqueducts, sewers, or other urban developments accelerate AMD formation even more, together with the rupture surfaces caused by MMs, as described in Section 5.5.

In relation to spontaneous ignition, the causative factor is hydrogen sulfide (H_2S , a highly flammable and toxic gas) in high content, related to the lithology and type of macerals. Therefore, for the Paja Formation, this great biogenic contribution is very possibly related to a bloom of brown algae (topic under investigation), which, according to [66], are called harmful algal blooms or HABs. The smoke and gases originating from these fossil algae are toxic in high concentrations or long exposures. It has been shown that this type of combustion is at low temperatures (specifically, low-temperature oxidation [50]), the

flames of which can burn in coal or black shale, peat, melted permafrost, and other organic matter for months or even years, as has been reported in recent years in the arctic circle [67], which dramatically contributes to climate change.

Both the texture (although fine and granular), as well as composition (minerals and organic content) and structure, reflect a high variability at the regional level (based on the secondary information evaluated), which indicate abundant carbonate facies, abundant microfossils, fish, mollusks (in our case, only cephalopods, typically small and immature), and other predatory mammalian fossils [68–70] in the Andean marine transgression at the end of the Mesozoic Era, but which are absent within the lithosequence evaluated (urban area of the municipality of Vélez, Santander).

Regarding provenance and the sedimentary depocenter, due to the quartz, mica, feldspar, heavy and clay minerals content, we share the statement of [71] that the Cretaceous strata of Colombia are primarily composed of siliciclastic sediments derived from the Guyana Shield to the east and, at times, from the ancestral Central Cordillera to the west, inside a continental transtensional regime. Therefore, Kip had a sedimentary origin and continuous depositional system in the warm marine environments of the Lower Cretaceous (~120–113 My) from shallow basins in the Sea of Tethys, which connected large oceans from east to west [18]. Different mechanisms can occur in the sedimentary environment, ones include changes in precipitation and evaporation rates, sea-level fluctuations, and increasing productivity (improved organic matter flow, followed by strongly restricted ventilation and high residence time) [72]. These indelible traces mark the character of the rock; all of this, together with lithification–diagenesis, gives the mudstones a unique imprint in terms of textural, structural, and compositional features, which are then exhumed and subjected to denudation processes (weathering, erosion, and MMs), generating the evaluated local–regional geohazards.

7. Conclusions

The lithified sediments of the Paja Formation are made up of a sand-sized felsic siliciclast sequence and a very dominant particulate combination of gray to black silts and clays, lithified into various crystalline phases with a strong biogenic signature. For this reason, they have been called bituminous mudstones (organic-rich mudstones), which are found in massive and very thick beds, with a powerful and almost monotonous sequence, in addition to being not fully laminated (dominantly wavy and lenticular lamination, not parallel and always discontinuous, scarcely flat-parallel) and locally fissile (only in heavily weathered outcrops).

Within the urban area of Vélez, it reaches an accumulated thickness of 99 m and is made up of four biolithostratigraphic segments (dominant muddy facies), rich in silicates, sulfides, and organic matter and with centimetric nodules in almost the entire column. A broad gypsum facies is at the base, with another thin medium sandy facies at the top (lenticular, very ferric), and on top of that, nodular layers of sporadic siderite, tending towards grain growth. Subsequently, they are lithified and probably have low-grade metamorphism (and/or high diagenesis) due to the abundant pyrophyllite and chlorites [48].

The Paja Formation was accumulated during the Aptian age of the Lower Cretaceous, under conditions that were not shallow but offshore and highly sulfurous and ferruginous [18], defined as euxinic by the presence of framboidal pyrite ($\cong 5 \mu\text{m}$), with its particular organic components and non-crystalline phases [19]. We also consider that an OAE can be chemostratigraphically ($\delta^{13}\text{C}$) defined, in line with [73].

Regarding the phenomena evaluated (slides–creep–subsidence, hydrogeochemical dynamism, rare earths, and spontaneous ignition), it is worth noting that:

- (a) *Hydrogeochemical reactivity*, *MM*, and *spontaneous combustion* are closely related to the intense weathering processes, dominant in Vélez: higher ratios of surface area to volume (SA:V) produce higher rates of overall weathering, driven exogenously by high relative humidity and favorable climatic and altitudinal conditions (which change in very short times), changing the petrophysical properties of the rock mass

and dramatically and extensively increasing the microporosity and, in turn, the permeability (or storage and flow capacities, respectively) of these rocks, which are not entirely aquitards. This condition alters the stress–strain state in 3D (greater friability, less resistance–stiffness of the mudstone) and prolongs the activity and geochemical intensity over time. All this reduces the cohesion and angle of internal friction, which causes slow deformations (e.g., soil creep), increasing the terrain susceptibility to other MMs (landslides, flows, wedge or block slides), especially in the contacts between rock and colluvium or the shallow weathering rock profiles (regoliths, little developed by the said morphodynamics).

- (b) *Spontaneous ignition*, together with the presence of REEs and natural radioactivity, are geochemical phenomena that must be mapped and monitored for the correct prevention or mitigation as well as water remediation contaminated with sulfuric acid (H_2SO_4), flowing freely in the urban sector. Unfortunately, spontaneous ignition occurs in the rural area of Vélez.

This way, the petrophysical properties and geochemistry can be mapped on a detailed scale: innovative, inherent, or causal contributing factors, not only internal ones, are, today, of great interest to researchers in hazard zoning studies on intertropical mountain slopes or anthropic cuts for urban planning or engineering works [18,33–35].

Finally, shales must be demystified (from their own conceptualization to knowing their true susceptibility and implications as geohazards) by turning them into the subject–object of more comprehensive scientific studies [36]. These challenges must be assumed by engineering, environmental, natural, and social sciences and prioritized in local communities at risk, contributing to a more resilient society with sustainability, stability, security, and integrity.

Author Contributions: Conceptualization, methodology, investigation, formal analysis, writing—review and editing, supervision, project administration, funding acquisition, G.A.R.-M.; methodology, formal analysis, validation, writing, research support, J.A.H.-M.; conceptualization, investigation, visualization, writing—review, E.C.M. All authors have read and agreed to the published version of the manuscript.

Funding: This research was directly funded by G.A. Reyes-Mendoza, between the years 2016 to 2021, in terms of travel expenses (national to local), food and lodging, stationery, materials and geological field instruments, rental of manual tools and other supplies, together with office expenses and editorials, as part of the doctoral thesis in Earth Sciences that is being prepared, and will be deposited and defended by the doctoral student before the UB in the second semester of 2023. Contributions in kind of the UIS, through the director of the Geomatics Group and the director from the School of Civil Engineering, provided support in administrative management to access the various institutional laboratories, equipment, tests, and the use of digital information (i.g. cartographic, geophysical and geotechnical) available from previous studies, in which the author participated.

Institutional Review Board Statement: Not applicable.

Informed Consent Statement: Not applicable.

Data Availability Statement: Not applicable.

Acknowledgments: The authors thank the staff of Guatiguará Technology Park (PTG), as part of the Industrial University of Santander, located at Piedecuesta Campus, the directors of the LGP Petroleum Geochemistry and LabMIC microscopy laboratories of the School of Geology, and the spectroscopy laboratory of the School of Physics. Additional thanks are given to the sample preparation and petrography laboratories and to the soil chemical laboratory on the main Bucaramanga campus. They also thank the IGAC National Soil Laboratory, Bogotá headquarters, for the preparation of regolith and colluvium samples in thin sections and for providing a microscope for micromorphological interpretation. The main author especially thanks the engineer MSc Wilfredo del Toro Rodríguez for his kind collaborations.

Conflicts of Interest: The authors declare no conflict of interest.

References

1. Harper, D.S. Etymology Dictionary; 2001, updated on 6 August 2022. Available online: <https://www.etymonline.com/word/shale> (accessed on 20 August 2022).
2. Oxford University Press. Definition of Shale Noun. In *Oxford Advanced American Dictionary*; June 2022. Available online: https://www.oxfordlearnersdictionaries.com/definition/american_english/shale (accessed on 10 August 2022).
3. Sherwin, G.A. A Kimmeridge shale dish. Society of Antiquaries of London. Society of Antiquaries of London. *Antiqu. J.* **1936**, *16*, 202–203. Cambridge University Press; 8 January 2012. Available online: <https://www.cambridge.org/core/j> (accessed on 7 August 2022). [CrossRef]
4. Gallois, R.; Etches, E. The stratigraphy of the youngest part of the Kimmeridge Clay Formation (Upper Jurassic) of the Dorset type area. *Proc. Geol. Assoc.* **2001**, *112*, 169–182. [CrossRef]
5. Wilkins, A.D. *Terminology and the Classification of Fine Grained Sedimentary Rocks—Is There a Difference between a Claystone, a Mudstone and a Shale?* Department of Geology and Petroleum Geology, University for Aberdeen: Aberdeen, UK, 2010; 12p.
6. Lindner, E. *Review of the Effects of CO₂ on very-Fine-Grained Sedimentary Rock/Shale. Part I: Problem Definition*; Technical Report Series; U.S. Department of Energy, National Energy Technology Laboratory (NETL): Morgantown, WV, USA, 2016; 68p.
7. Tourtelet, H.A. Origin and use of the word “shale”. *Am. J. Sci.* **1960**, *258*, 35–343.
8. Boggs, S., Jr. *Petrology of Sedimentary Rocks*, 2nd ed.; Cambridge University Press: New York, NY, USA, 2009; 599p.
9. Potter, P.E.; Maynard, J.B.; Depetris, P.J. *Mud and Mudstones. Introduction and Overview*; Springer: Berlin/Heidelberg, Germany, 2005; 297p.
10. Gallegos, J.A. Clasificación de las rocas sedimentarias: Sugerencias para su aprendizaje. *Enseñanza Cienc. Tierra* **1995**, *3.3*, 154–163.
11. Lazar, O.R.; Bohacs, K.M.; Macquaker, J.H.S.; Schieber, J.; Demko, T.M. Capturing key attributes of fine-grained sedimentary rocks in outcrops, cores, and thin sections: Nomenclature and description guidelines. *J. Sediment. Res.* **2015**, *85*, 230–246. [CrossRef]
12. Reyes, M.G.A. Evaluación detallada e impacto de rocas lodosas meteorizadas. El caso de Vélez (Santander, Colombia). In *XIII Semana Técnica de Geología, Ingeniería Geológica y Geociencias*; Universidad de Caldas: Manizales, Colombia, 2018; 3p.
13. Abelleira, M. *El Boom del Shale en Estados Unidos (2008–2017). Proyecto de Investigación*; Universidad Nacional de Quilmes, Departamento de Economía y Administración, Licenciatura en Economía del Desarrollo: Bernal, Argentina, 2020; 34p.
14. Blatt, H.; Middleton, G.; Murray, R. *Origin of Sedimentary Rocks*, 2nd ed.; Prentice-Hall Inc.: Englewood Cliffs, NJ, USA, 1972; 643p.
15. Schieber, J.; Bose, P.K.; Eriksson, P.G.; Banerjee, S.; Sarkar, S.; Altermann, W.; Catuneanu, O. (Eds.) *Atlas of Microbial Mat Features Preserved within the Siliciclastic Rock Record*; Atlases in Geoscience; Elsevier: Amsterdam, The Netherlands, 2007; 311p.
16. Li, W.; Liu, Y.; Xiao, S.; Zhang, Y.; Chai, L. An investigation of the underlying evolution of shale gas research’s domain based on the co-word network. *Sustainability* **2018**, *10*, 164. [CrossRef]
17. Potter, P.E.; Maynard, J.B.; Pryor, W.A. *Sedimentology of Shale: Study Guide and Reference Source*; Springer: Berlin/Heidelberg, Germany, 1980; 303p.
18. Reyes-Mendoza, G.A. Manodisciplines applied to understand the complexity of mudstones and its links with the instability of slopes: Interrelationships between endogenous and exogenous contributing factors, weathering agents & dynamics, next to other environmental considerations. In *Modern Concepts in Material Science*; Iris Publishers: San Francisco, CA, USA, 2021; Volume 4, 3p.
19. Upscaling geoenvironmental analysis, thematic mapping and nanotechnological characterization combined in bituminous mudstone outcrops studies, Eastern Cordillera, Colombian Northern Andes: Application in detailed zoning of susceptibility to mass movements. In Proceedings of the 3rd International Webinar on Material Science and Nanotechnology, Peers Alley Media, Paris, France, 16 September 2021; 2p.
20. Ghadeer, S. An Investigation of the Sediment Dispersal Operating to Control Lithofacies Variability and Organic Carbon Preservation in an Ancient Mud-Dominated Succession: A Case Study of the Lower Jurassic Mudstone Dominated Succession Exposed in the Cleveland Basin. Ph.D. Thesis, School of Earth, Atmospheric, and Environmental Sciences, University of Manchester, Manchester, UK, 2011; 169p.
21. Kansas Geological Survey. Organic Mudstones. 24 March 2017. Available online: https://www.kgs.ku.edu/Publications/Bulletins/LA/10_mudstones.html%20Organic%20Mudstones (accessed on 5 February 2018).
22. Taylor, G.H.; Teichmüller, M.; Davis, A.; Diesel, C.F.K.; Littke, R.; Robert, P. *Organic petrology. A New Handbook Incorporating Some Revised Parts of Stach’s Textbook of Coal Petrology*; Gebrüder Borntraeger: Stuttgart, Germany, 1998; 704p.
23. Schieber, J. *Black Shales. Encyclopedia of Sediments and Sedimentary Rocks*; Middleton, G.V., Ed.; Kluwer Scientific Publishers: Dordrecht, The Netherlands; Boston, MA, USA, 2003; Chapter B; 3p.
24. Potter, P.E.; Maynard, J.B.; Pryor, W.A. *Sedimentology of Shale. Study Guide and Reference Source*, 2nd ed.; Springer Science & Business Media: New York, NY, USA, 2012; 310p.
25. Putera, A.M.A.; Pramusandi, S.; Damianto, B. Identification and classification of clayshale characteristic and some considerations for slope stability. *Afr. J. Environ. Sci. Technol.* **2017**, *11*, 163–197. [CrossRef]
26. Schieber, J.; Lazar, R.; Bohacs, K.; Klimentidis, B.; Dumitrescu, M.; Ottmann, J. An SEM study of porosity in the Eagle Ford Shale of Texas—Pore types and porosity distribution in a depositional and sequence stratigraphic context. *Am. Assoc. Pet. Geol.* **2016**, *110*, 167–186.
27. Garum, M.; Glover, P.W.J.; Lorinczi, P.; Drummond-Brydson, R.; Hassanpour, A. Micro- and nano-scale pore structure in gas shale using X_μ-CT and FIB-SEM techniques. *Energy Fuels* **2020**, *34*, 12340–12353. [CrossRef]

28. Fleming, R.W.; Spencer, G.S.; Banks, D. Empirical study of behavior of clay shale slopes. *U.S. Army Eng. Nucl. Cratering Group. NCG Tech. Rep.* **1970**, *1*, 103.
29. Energy Information Administration — EIA. *Technically Recoverable Shale Oil and Shale Gas Resources: An Assessment of 137 Shale Formations in 41 Countries Outside the United States*; U.S. Department of Energy: Washington, DC, USA, 2013; 76p.
30. Slatt, R.M.; Zhang, J.; Torres-Parada, E.; Brito, R.; Duarte, D.; Milad, B. Rock Mechanics in Unconventional Shales. Volume 5, Geological Resources, Energy. In *Encyclopedia of Geology*, 2nd ed.; Scott, E., David, A., Eds.; Elsevier B.V. Science Direct: Amsterdam, The Netherlands, 2021; pp. 783–807.
31. Geomática, Gestión y Optimización de Sistemas. Estudio de Amenaza, Vulnerabilidad y Riesgo por Movimientos en Masa del Municipio de Vélez, Departamento de Santander. Volumen II-A. In *Convenio Interadministrativo No. 9677-04-1127-2013 Celebrado Entre la Unidad Nacional de Gestión del Riesgo de Desastres, el Departamento de Santander, el Municipio de Vélez y la Universidad Industrial de Santander—Escuela de Ingeniería Civil*; Geomática, Gestión y Optimización de Sistemas: Bucaramanga, Colombia, 2015; 270p.
32. *Estudio de Amenaza, Vulnerabilidad y Riesgo por Movimientos en Masa en el Municipio de Vélez*; Publicaciones Universidad Industrial de Santander: Bucaramanga, Colombia, 2017; 180p.
33. Reyes, M.G.A. Zonificación de amenazas por deslizamientos: Métodos, resultados y retos para la gestión del riesgo en el caso de Vélez (Santander). In *Proceedings of the 1er Simposio Internacional de Geotecnia Ambiental y Gestión del Riesgo de Desastres*. Universidad de Santander, Especialización en Geotecnia Ambiental, Bucaramanga, Colombia, 7 April 2017.
34. *Morfodinámica de Rocas Lodosas en Ambientes Intertropicales: Problemática, Caracterización Detallada, Meteorización, Susceptibilidad a Movimientos en Masa y Otras Implicaciones Ingenieriles*; Universidad la Gran Colombia, Decanatura de la Facultad de Ingeniería: Bogotá, Colombia, 2018.
35. Las rocas lodosas de Vélez: De la meteorización a los deslizamientos. In *Fest Station-Intelligent UIS, Seminario U18 Fest-Ideas para transformar el mundo*; Presentación Oral; Universidad Industrial de Santander: Bucaramanga, Colombia, 2019.
36. Aciertos y Desaciertos en el Conocimiento de los Movimientos en Masa en Vélez, Departamento de Santander. ¿Por qué falla su Gestión? En *Conversatorio Virtual ‘Movimientos en Masa: Estudios de caso e Importancia en la Toma de Decisiones en el OT [Online]*. Unidad Nacional para la Gestión del Riesgo de Desastres. Bogotá, Mayo de 2021. Available online: <https://www.youtube.com/watch?v=C8VkJtuwMPcQ> (accessed on 7 July 2021).
37. McCourt, W.J.; Aspaden, J.A.; Brook, M. New geological and geochronological data from the Colombian Andes: Continental growth by multiple accretion. *J. Geol. Soc.* **1984**, *141*, 831–845. [[CrossRef](#)]
38. Taboada, A.; Rivera, L.A.; Fuenzalida, A.; Cisternas, A.; Philip, H.; Bijwaard, H.; Olaya, J.; Rivera, C. Geodynamics of the northern Andes: Subductions and intracontinental deformation (Colombia). *Tectonics* **2000**, *19*, 787–813. [[CrossRef](#)]
39. Trenkamp, R.; Kellogg, J.; Freymueller, J.; Mora, H. Wide plate margin deformation, southern Central America and northwestern South America, CASA GPS observations. *J. South Am. Earth Sci.* **2002**, *15*, 157–171. [[CrossRef](#)]
40. Jara, J.J.; Barra, F.; Reich, M.; Leisen, M.; Romero, R.; Morata, D. Episodic construction of the early Andean Cordillera unravelled by zircon petrochronology. *Nat. Commun.* **2021**, *12*, 4930. [[CrossRef](#)]
41. Ramos, V. Anatomy and global context of the Andes: Main geologic features and the Andean orogenic cycle. *Geol. Soc. Am.* **2009**, *204*, 31–65.
42. Spikings, R.; Van der Lelij, R. The geochemical and isotopic record of Wilson Cycles in Northwestern South America: From the Iapetus to the Caribbean. *Geosciences* **2021**, *12*, 5. [[CrossRef](#)]
43. Cortés, M.; Angelier, J. Current states of stress in the northern Andes as indicated by focal mechanisms of earthquakes. *Tectonophysics* **2005**, *403*, 59–75. [[CrossRef](#)]
44. Reyes, M.G.A.; y Flórez, O.H.D. *Geología Urbana de Barrancabermeja 2022. Geociencias en las Fronteras de la Sostenibilidad Territorial*; Mojica Asoc. Impr. Sas: Bucaramanga, Colombia, 2022; 70p.
45. Suter, F.; Sartori, M.; Neuwerth, R.; Gorin, G. Structural imprints at the front of the Chocó-Panamá indenter: Field data from the North Cauca Valley Basin, Central Colombia. *Tectonophysics* **2008**, *460*, 134–157. [[CrossRef](#)]
46. Ariza-Acero, M.M.; Spikings, R.; Beltran-Triviño, A.; Ulianov, A.; von Quadt, A. Geochronological, geochemical and isotopic characterisation of the basement of the Chocó-Panamá Block in Colombia. *Lithos* **2022**, *412–413*, 106598. [[CrossRef](#)]
47. Gómez, J.; Núñez-Tello, A.; Alcárcel, F.A.; Mateus-Zabala, D.; Pinilla-Pachón, A.O.; Lasso-Muñoz, R.M.; Marín-Rincón, E.; Montes-Ramírez, N.E. Chapter 1 Physiographic and geological context of the Colombian Territory. In *The Geology of Colombia, Volume 1 Proterozoic—Paleozoic*; Gómez, J., Mateus-Zabala, D., Eds.; Servicio Geológico Colombiano, Publicaciones Geológicas Especiales: Bogotá, Colombia, 2020; pp. 1–16.
48. Ríos-Reyes, C.A.; Reyes-Mendoza, G.A.; Henao-Martínez, J.A.; Williams, C.; Dyer, A. First report on the geologic occurrence of natural Na–A zeolite and associated minerals in cretaceous mudstones of the Paja Formation of Vélez (Santander), Colombia. *Crystals* **2021**, *11*, 218. [[CrossRef](#)]
49. Sullivan, P.L.; Hynek, S.A.; Gu, X.; Singha, K.; White, T.; West, N.; Kim, H.; Clarke, B.; Kirby, E.; Duffy, C.; et al. Oxidative dissolution under the channel leads geomorphological evolution at the Shale Hills catchment. *Am. J. Sci.* **2016**, *316*, 981–1026. [[CrossRef](#)]
50. West, I.M. *Kimmeridge Oil Shale, the Blackstone, at Clavell’s Hard*. iSolutions [Online], Faculty of Natural and Environmental Science of the Southampton University, August 2016. Available online: www.southampton.ac.uk/~jimw/Kimmeridge-Oil-Shale.htm (accessed on 10 June 2022).

51. Gao, P.; Liu, G.; Jia, C.; Li, C.; Zhang, P.; Sun, R. REE Geochemistry of organic fractions in mudstone source rock and oil sand from Aer Sag, Erlian Basin: Implications for oil-source correlation. Abstract. In Proceedings of the AAPG Annual Convention and Exhibition, Denver, CO, USA, 3 June 2015; 1p.
52. Castro, M.E. Concepto técnico sobre un deslizamiento en el sitio Guayabal, vereda Loma Alta, municipio de Vélez, departamento de Santander. *Ingeominas* **2009**, 1–15.
53. *Combustión Espontánea de Arcillolitas Carbonosas en el Municipio de Simacota, Departamento de Santander*; Servicio Geológico Colombiano: Bucaramanga, Colombia, 2017; 25p.
54. Restuccia, F.; Ptak, N.; Rein, G. Self-heating behavior and ignition of shale rock. *Combust. Flame* **2017**, *176*, 213–219. [[CrossRef](#)]
55. Tang, Y. A laboratorial study of spontaneous combustion characteristics of the oil shale in Fushun, China. *Combust. Sci. Technol.* **2016**, *188*, 997–1010. [[CrossRef](#)]
56. Liu, H.P.; Lv, Z.W.; Wang, X.; Zhang, S.Q.; Wang, Z.C.; Wang, Q. Study on spontaneous combustion characteristics and risk of oil shale. Abstract. *Combust. Sci. Technol.* **2022**, 1p. [[CrossRef](#)]
57. Krinsley, D.H.; Pye, K.; Boggs, S., Jr.; Tovey, N.K. *Backscattered Electron Microscopy and Image Analysis of Sediments and Sedimentary Rocks*; Cambridge University Press: Cambridge, UK, 1998; 193p.
58. Gao, F.; Song, Y.; Lia, Z.; Xionge, F.; Chena, L.; Zhangf, X.; Chena, Z.; Moortgat, J. Quantitative characterization of pore connectivity using NMR and MIP: A case study of the Wangyinpu and Guanyintang shales in the Xiuwu basin, Southern China. *Int. J. Coal Geol.* **2018**, *197*, 53–65. [[CrossRef](#)]
59. Geoscience.blog. What is the Relationship between Total Pore Space and Texture? [Online] Our Planet Today, 16 April 2022. Available online: <https://geoscience.blog/what-is-the-relationship-between-total-pore-space-and-texture/> (accessed on 3 January 2023).
60. Sun, M.; Zhao, J.; Pan, Z.; Hu, Q.; Yu, B.; Tan, Y.; Sun, L.; Bai, L.; Wu, C.; Blach, T.P.; et al. Pore characterization of shales: A review of small angle scattering technique. *J. Nat. Gas Sci. Eng.* **2020**, *78*, 103294. [[CrossRef](#)]
61. Bennett, R.H.; Bryant, W.R.; Hulbert, M.H.; Chiou, W.A.; Faas, R.W.; Kasproiwicz, J.; Li, H.; Lomenick, T.; O'Brien, N.R.; Pamukcu, S.; et al. Microstructures of fine-grained sediments. From mud to shale. In *Frontiers in Sedimentary Geology*; Bouma, A.H., Ed.; Springer Science & Business Media: New York, NY, USA, 1991; Volume III, 582p.
62. Shapiro, A.M.; Evans, C.E.; Hayes, E.C. Porosity and pore size distribution in a sedimentary rock: Implications for the distribution of chlorinated solvents. *J. Contam. Hydrol.* **2017**, *203*, 70–84. [[CrossRef](#)]
63. Slatt, R.M.; O'Brien, N.; Molinares-Blanco, C.; Serna-Bernal, A.; Torres, E.; Philp, P. Pores, spores, pollen and pellets: Small, but significant constituents of resource shales. In Proceedings of the Unconventional Resources Technology Conference-URTEC 1573336, Denver, CO, USA, 12–14 August 2013; 13p.
64. Winnick, M.J.; Carroll, R.W.H.; Williams, K.H.; Maxwell, R.M.; Dong, W.; Maher, K. Snowmeltcontrols on concentration-dischargerelationships and the balance ofoxidative andacid-base weathering fluxes in analpine catchment, East River, Colorado. *Water Resour. Res.* **2017**, *53*, 2507–2523. [[CrossRef](#)]
65. Winnick, M.J. Shale Weathering. Coupled Oxidation of Pyrite and Dissolution of Carbonate in Sales. In M. W. blog Environmental Geochemistry, Past and Present. Proudly Powered by WordPress, Expound by Konstantin Kovshenin, Department of Geosciences at the University of Massachusetts Amherst. Without Date. Available online: <https://blogs.umass.edu/mwinnick/shale-weathering-2/> (accessed on 10 June 2022).
66. NOAA. What Is a Harmful Algal Bloom? Sometimes Tiny Algae can Cause Big Problems. The National Oceanic and Atmospheric Administration, United States Department of Commerce. [Online] NASA, 27 April 2016. Available online: <https://www.noaa.gov/what-is-harmful-algal-bloom> (accessed on 20 July 2022).
67. Witze, A. *Why Arctic Fires Are Bad News for Climate Change*; Springer: Berlin/Heidelberg, Germany, 2020; Volume 585, pp. 336–337.
68. Gómez-Gutiérrez, J.C.; Páramo-Fonseca, M.E. Nuevos Restos de Pliosaurio Encontrados en Rocas del Cretácico Inferior de Villa de Leiva, Boyacá. In Proceedings of the XIV Colombian Congress of Geology and I Symposium of Explorers, Bogotá, Colombia, 1 August 2013; 1p.
69. Gómez-Pérez, M.; Noé, L.F. Cranial anatomy of a new pliosaurid *Acostasaurus pavachoquensis* from the Lower Cretaceous of Colombia, South America. *Palaeontogr. Abt. A* **2017**, *310*, 5–42. [[CrossRef](#)]
70. Noé, L.F.; Gómez-Pérez, M. Giant pliosaurids (Sauropterygia; Plesiosauria) from the Lower Cretaceous peri-Gondwanan seas of Colombia and Australia. *Cretac. Res.* **2021**, *132*, 105–122.
71. Villamil, T. Chronology relative sea level history and a new sequence stratigraphic model for basinal Cretaceous facies of Colombia. In Proceedings of the Society for Sedimentary Geology (SEPM), El Paso, TX, USA, June 2012; pp. 161–216.
72. Herrle, J.O.; Kössler, P.; Bollmann, J. Palaeoceanographic differences of early Late Aptian black shale events in the Vocontian Basin (SE France). *Palaeogeogr. Palaeoclimatol. Palaeoecol.* **2010**, *297*, 367–376. [[CrossRef](#)]
73. Silva, J.C. Sedimentological and geochemical expression of the anoxic oceanic events of the Cretaceous in Colombia, an unconventional vision. In *Wednesday of Geology*; Oral Presentation; Colombian Geological Service, Benjamín Alvarado Auditorium: Bogotá, Colombia, 2018.

Disclaimer/Publisher's Note: The statements, opinions and data contained in all publications are solely those of the individual author(s) and contributor(s) and not of MDPI and/or the editor(s). MDPI and/or the editor(s) disclaim responsibility for any injury to people or property resulting from any ideas, methods, instructions or products referred to in the content.